Phase-noise scaling in quantum soliton propagation

R. M. Shelby
IBM Research Division, Almaden Research Center, 650 Harry Road, San Jose, California 95120-6099

P. D. Drummond and S. J. Carter
Department of Physics, University of Queensland, St. Lucia, Queensland, Australia 4067
(Received 27 November 1989)

We treat the scaling of thermal phase-noise effects and quantum fluctuations for solitons in optical fibers. The central result is that the size of the thermal noise relative to quantum noise is reduced in proportion to the soliton duration for solitons whose duration is less than the thermal correlation times, suggesting that squeezed quantum solitons should be realizable in optical fibers. The physical basis for this effect is largely the fact that squeezing, which is nonlinear, occurs more rapidly for shorter pulses.

I. INTRODUCTION

Squeezed light, in which fluctuations in one quadrature of the electromagnetic field are reduced to less than the vacuum or shot-noise limit, has been produced and detected in several different laboratory experiments.[1-4] This nonclassical light might be used to improve the signal-to-noise ratio in sensitive optical experiments, and perhaps in technological applications. Means of generation must still be developed that are simple, reliable, and that produce squeezing over a useful bandwidth. Optical parametric oscillators (OPO's) have shown themselves to be nearly ideal devices for the transformation of vacuum fluctuations into squeezed light,[2] but are still quite complicated and unreliable. Compact, monolithic, OPO's are currently being developed,[5] and these may one day result in a simple and inexpensive source of squeezed radiation. Semiconductor diode lasers, when pumped with a sub-Poissonian current source and operated many times above threshold, have been shown to directly generate an amplitude-squeezed state;[6] however, noise-generation mechanisms in these devices are poorly understood and are very sensitive to optical feedback.

In previous experiments, we have investigated the squeezing of light by self-phase-modulation in single-mode optical fiber.[3] It was believed at the outset that single-mode fiber could provide a low-loss, readily available, broadband nonlinear medium. Because the nonlinearity is nonresonant and electronic in origin, nearly ideal behavior was expected, with useful amounts of squeezing at easily attainable pump powers. However, excess phase noise partially obscured the squeezed quadrature, and less than 20% squeezing was observed. This excess noise originates from thermally induced fluctuations in the fiber refractive index. The observed thermal noise arises from two different origins: a structured spectrum from acoustic waves confined by the cylindrical fiber geometry [guided-acoustic-wave Brillouin scattering[7] (GAWBS)] and a power-law spectrum from thermally activated relaxational modes of the amorphous silica matrix.[8] The latter mechanism, essentially $1/f$ noise in the refractive index of the fiber, was the limiting one in cw squeezing experiments, and our recent investigations have led to a more thorough understanding of its origin and to new knowledge of the microscopic structure of fused silica. However, cooling the fiber to liquid-helium temperatures was not sufficient to reduce this noise to an insignificant level relative to the vacuum noise, subject to the constraints of limited pump power due to stimulated Brillouin scattering.[3]

The extent to which thermal phase noise limits squeezing can be characterized by a parameter proportional to the ratio of the light-scattering cross section to the effective fiber nonlinearity. One approach to reduce this ratio is to consider the use of a train of short pulses, e.g., from a mode-locking laser.[9-11] Distortion of the pump pulses due to self-phase-modulation and group velocity dispersion led us to consider pump pulses in the form of optical solitons.[12] The high peak power of these pulses should increase the effective nonlinearity and thus reduce the length of fiber needed to produce squeezing. On the other hand, the spectrum of phase noise for pulses will, roughly speaking, be the convolution of the pulse spectrum and the spectrum of refractive-index fluctuations, and the relative bandwidth of the refractive-index noise and the pulse is an additional important parameter. The main goal of this paper is to discuss qualitatively how the phase noise and nonlinear effects should be expected to scale with pulse width and to present quantitative results obtained from detailed computer modeling of the propagation of quantum noise and thermal phase noise associated with a soliton pulse. We find in the limit that the pulse bandwidth is large (i.e., the pulse short) relative to the refractive-index noise bandwidth, squeezing performance improves as the pulses are shortened further, and squeezing of quantum noise by a factor of ten should be obtainable after propagation of a few soliton periods.

II. THERMAL PHASE NOISE IN OPTICAL FIBERS

A. Introduction

We have investigated in detail light-scattering processes in fused silica optical fibers for frequencies between 100 kHz and 1 GHz.[7,8] Guided-acoustic-wave Brillouin scattering (GAWBS) produces a structured phase-noise spectrum beginning near 20 MHz and extending beyond our instrumental cutoff of 1 GHz. Phase-noise peaks are observed, corresponding to the resonant modes of an elastic cylinder (i.e., the fiber).[7] The light-scattering spectrum for a typical plastic-jacketed fiber is shown in a schematic fashion in Fig. 1. The figure was based on our own extensive experimental investigation of low-frequency thermal phase noise in silicon fibers, our theoretical knowledge and physical intuition regarding how this noise should behave, as well as on information in the literature on light scattering in glass. The vertical scale in this figure corresponds to a scattering cross section normalized to be independent of measurement bandwidth and numerical aperture of the fiber (the solid angle of collection). This is done by normalizing the mean-square optical field due to light scattering to the mean-square vacuum-noise field for the same spatial mode and measurement bandwidth, leading to a noise power spectral density measured in vacuum-noise units, or VNU.[13,14] The scattering is also proportional to the pump power and fiber interaction length. The peaks above 10 MHz are due to GAWBS and are assumed to broaden toward higher frequencies because of damping of the fiber elastic modes by the plastic fiber jacket, and also because of variations in the fiber diameter. Above a few hundred MHz the peaks tend to merge, leading to a relatively structureless spectrum. The GAWBS is believed to have a cutoff frequency at about the point where the acoustic wavelength becomes small compared with the size of the confined optical mode, taken as 20 GHz for this figure. This cutoff has not yet been verified experimentally.

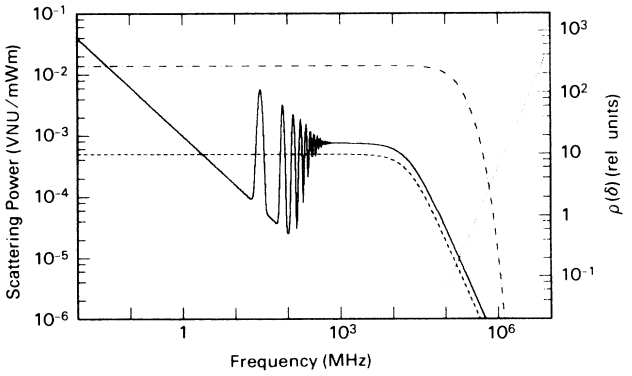

FIG. 1. The solid curve shows a schematic representation of the absolute light-scattering cross section for fused silica optical fiber. The left vertical axis gives the scattered noise power relative to the vacuum noise (i.e., in vacuum-noise units, or VNU) for 1 mW of pump power and 1 m of fiber. The right vertical axis shows the corresponding phase-noise coefficient $\rho(\delta)$, assuming a typical value for the Kerr coefficient. The dashed curve is the Lorentzian approximation to the phase-noise spectrum assumed for the numerical simulations (drawn here for $g=10$). The dotted curve shows the onset of Raman scattering by localized phonons. The dot-dashed curve is a representation (arbitrarily scaled for this figure) of the spectrum of a hyperbolic secant soliton pulse corresponding to phase-noise width $\gamma=0.1$ (see text).

Glasses are nonequilibrium materials, and the complex potential surface for the accessible configuration space of the glass is often modeled as a distribution of double-well potentials or so-called "two-level modes" (TLM).[15] Fluctuations in the refractive index result from the relaxational motions of groups of atoms modeled by thermal hopping over the barrier of the two-level mode. The low-frequency phase noise originates from these refractive-index fluctuations.[8] The mean time to hop from one well to the other for a particular local group of atoms is given by $\tau(E,T)=\tau_0\exp(E/kT)$, where E is the barrier height which is distributed according to the function $D(E)$, and τ_0 is an attempt time $\sim 10^{-13}$ sec. Each scattering center produces a Lorentzian spectrum, yielding an overall power spectrum:[8,16]

$$S(\omega,T)\propto T^{1.3}\int D(E)\frac{\tau(E,T)}{1+\omega^2\tau^2(E,T)}dE\ . \tag{2.1}$$

By fitting the observed temperature and frequency dependence of the phase-noise spectrum, we have determined that $D(E)=\exp(-E/E_0)$, where $E_0/k\sim 350^\circ$ K, and varies somewhat depending on glass composition. The phase noise has a power-law spectrum and a temperature dependence with a maximum at about 80 K, given by

$$S(\omega,T)\propto\frac{T^{2.3}(\omega\tau_0)^{kT/E_0}}{\omega}\ . \tag{2.2}$$

Recent measurements[13] have shown that this light scattering is quite highly polarized, with a polarization ratio on the order of 10. The spectrum has been investigated thoroughly for backscattering[8] and shown to have the form of equation (2) from below 100 kHz, where laser noise and microphonic pickup by the fiber become dominant, to over 100 MHz, where vacuum noise limits our ability to extract accurately the thermal noise contribution. Polarized and depolarized measurements confirm the presence of this noise in forward scattering, although the spectrum is partially obscured by the presence of the GAWBS peaks, beginning at about 15 MHz for typical fibers. An additional background contribution which cannot be accounted for by simple superposition of GAWBS and TLM spectra, and which is not yet well understood, also appears in the forward direction. A full discussion of the phase-noise behavior of optical fibers is planned to be published elsewhere.[13]

The dotted curve in Fig. 1 shows the onset of spontaneous Raman scattering in fused silica. For pulses whose spectra are sufficiently broad, the Raman scattering can be expected to add significant classical excess noise. We are not aware of any experimental investigations of excess noise on short pulses due to spontaneous Raman scattering, and the pulse width at which this noise becomes comparable to the vacuum noise is not known.

B. Scaling properties

In this section we wish to examine the scaling of the thermal-noise effects in a qualitative way. It is useful to start with a relatively simple model that gives the principle scaling behavior, deferring until later the discussion of the details of the thermal-noise spectrum. In previous papers,[12] we have demonstrated that a quantum soliton can give rise to a squeezed output field, given a coherent input. In reality this gives the minimal behavior that is compatible with quantum mechanics. The results obtained in a laboratory experiment will also include phase noise due to the environment of the nonlinear medium. In the case of quantum-optical solitons, the phase noise is well described by thermal fluctuations in the refractive index.

In order to show how these effects scale, we initially suppose that the linear fluctuations can be effectively decoupled from the nonlinear interactions causing squeezing. In this limit, the fiber acts as a phase modulator. The induced variance in the transmitted phase will scale linearly with fiber length. Thus an input field $\mathcal{E}(t)$ is transformed to $\mathcal{E}(t)e^{i\theta(t)}$, where $\theta(t)=\langle\theta(t)\rangle+\Delta\theta(t)$. For simplicity, we assume in this section that $\langle\theta(t)\rangle=0$.

In the simplest prototype of a squeezing experiment, the output field is combined with an intense local oscillator, and the variance in the photo count is measured over a time interval t_0. For the present purposes, more complex measurement schemes will have similar behavior with respect to scaling. We therefore suppose that the local oscillator field is itself a soliton pulse of duration t_0. For this calculation, the local oscillator will, in fact, be treated just as a square pulse of duration t_0 and phase θ_0 relative to the signal-field output mean phase. Numerical simulations using a more realistic model will be discussed below.

In the semiclassical limit, the output intensity at the photodetector in units of photons per second is of the form

$$I(t)=|\mathcal{E}_0e^{i\theta_0}+\mathcal{E}(t)e^{i\theta(t)}|^2 . \tag{2.3}$$

Here we can always choose a reference phase such that $\theta_0=0$. If we suppose that the signal field $\mathcal{E}(t)$ is also of approximately uniform amplitude in the detector time interval of t_0, this result for $I(t)$ can be then simplified to

$$I(t)\simeq|\mathcal{E}_0|^2+2\mathcal{E}_0\mathcal{E}\cos[\theta(t)]+O(\mathcal{E}^2) . \tag{2.4}$$

The shot-noise variance V_s in a coherent field is equal to the total number of photons counted in the time t_0, i.e.,

$$V_s=|\mathcal{E}_0|^2t_0 . \tag{2.5}$$

Here we have neglected the small count rate of the signal field $\mathcal{E}$ and assumed that $\mathcal{E}_0$ includes any factors due to beam-splitter and photodetector efficiency. We note that in a squeezing experiment, the shot-noise variance can be canceled by the interference between $\mathcal{E}_0$ and $\mathcal{E}$, resulting in fluctuations below the shot-noise limit.

We now consider the additional fluctuations due to the phase-noise term in Eq. (2.4). This contributes an extra term in the intensity correlation function, given by

$$\langle\Delta I(t)\Delta I(t')\rangle=4|\mathcal{E}_0\mathcal{E}|^2\langle[\Delta\cos\theta(t)][\Delta\cos\theta(t')]\rangle . \tag{2.6}$$

On integrating over the detection time of t_0, we obtain an additional contribution to the detected photon-count variance of

$$\delta V=4|\mathcal{E}_0\mathcal{E}|^2\int_0^{t_0}\int_0^{t_0}\langle[\Delta\cos\theta(t)][\Delta\cos\theta(t')]\rangle dt\,dt' . \tag{2.7}$$

We note that $\theta(t)$ includes all of the phase fluctuations induced in a propagating signal that is detected during t_0. Next consider the behavior of δV for different observation times t_0 compared with the correlation time T_c of the phase noise. In general, quite complicated behavior will occur on intermediate and long time scales. However, if we suppose that $T_c\gg t_0$, which is the most interesting limit for investigating squeezing, then we obtain the result that

$$\delta V=4|\mathcal{E}_0\mathcal{E}|^2\langle[\Delta\cos\theta(t)]^2\rangle . \tag{2.8}$$

The quantity of interest is the relative size of the phase-noise variance δV compared with the shot noise V_s. Combining (2.5) and (2.8), we have

$$\frac{\delta V}{V_s}=4|\mathcal{E}|^2t_0\langle[\Delta\cos\theta(t)]^2\rangle . \tag{2.9}$$

However, Eq. (2.9) does not yet display all the scaling dependence required by the propagation of soliton pulses in optical fibers.

For a given pulse width, t_0, soliton pulses are associated with a characteristic photon number $\bar{n}$ and propagation distance z_0. The characteristic distance is given by $z_0=t_0^2|k''|$, where $k''=\partial^2k/\partial\omega^2$ is a measure of the group-velocity dispersion of the fiber. z_0 is the distance over which a pulse of width t_0 is significantly broadened by dispersion.[17] For soliton propagation, this linear dispersion is balanced exactly by nonlinear self-phase-modulation, requiring a characteristic intensity or photon number, $\bar{n}=|k''|/\chi t_0$, where χ is a measure of the third-order nonlinear susceptibility of the fiber. Thus, if the signal field $\mathcal{E}$ is a soliton, then it varies inversely with time duration t_0:

$$\mathcal{E}=\sqrt{T_s}/t_0 , \tag{2.10}$$

where $T_s=|k''|/\chi$ is the characteristic time for a one-photon soliton. Combining Eq. (2.9) with (2.10), we obtain the unpromising result that

$$\frac{\delta V}{V_s}=4(T_s/t_0)\langle[\Delta\cos\theta(t)]^2\rangle . \tag{2.11}$$

Noting that typically $T_s\gg t_0$, we see that this result predicts a larger phase-noise effect for shorter coherent soliton inputs. This has a straightforward physical explanation. The effect of phase noise is much greater on a large coherent signal than on a small coherent signal, in terms of quadrature amplitudes. Thus, since short-pulse

solitons have a greater amplitude [see Eq. (2.10)], they are more strongly perturbed by the effects of phase modulation.

In reality, this picture is unnecessarily pessimistic. The reason we are investigating phase noise is in order to determine its effect on a squeezing experiment. However, squeezing occurs on a distance scale characteristic of the nonlinear effects, which itself depends on intensity and is given by z_0. We expect the intrinsic phase-noise variance to scale linearly with z. Thus, at fixed scale distance, $\zeta=z/z_0$,

$$\langle \Delta\theta^2 \rangle = \alpha z_0 \zeta = \alpha t_0^2 \zeta / |k''| \ . \tag{2.12}$$

On linearizing with respect to $\Delta\theta$,

$$\frac{\delta V}{V_s} = 4\alpha\zeta \left[\frac{t_0}{\chi} \right] \sin^2\theta_0 \ . \tag{2.13}$$

Thus we see that for experiments at a given soliton interaction distance, ζ, the relative phase fluctuations are linearly proportional to the pulse duration t_0. This suggests that the use of pulses that are short relative to the correlation time of the thermal refractive-index fluctuations can minimize the impact of these fluctuations on a squeezing experiment. In the following sections we study the squeezing of soliton pulses in the presence of thermal phase noise in more detail and confirm these scaling ideas with numerical simulations.

III. NOISE ON SOLITON PULSE TRAINS

We anticipate that experimental measurements of quantum- and thermal-noise fluctuations on soliton pulses will be performed using a continuous train of picosecond pulses derived from a cw mode-locked laser. Such lasers have been employed in other squeezing experiments.[10,18] It has been demonstrated that the photocurrent power spectrum, resulting from the detection of such a pulse train, consists of a series of sharp spikes at multiples of the pulse repetition frequency, corresponding to the mean field of the pulses, and that at other frequencies, broadband noise is observed, corresponding to quantum fluctuations and excess classical noise.

We now consider the effect of thermal phase noise on such a periodic train of short pulses with repetition rate $\Delta\omega/2\pi$. The pump field, centered at frequency ω_0, can be written in terms of amplitudes ϕ_j:

$$E(\tau) = \sqrt{\bar{n}\Delta\omega/2\pi}\, e^{-i\omega_0\tau} \sum_j \phi_j e^{-ij\Delta\omega\tau} \ . \tag{3.1}$$

The ϕ_j are normalized, such that $\sum_j |\phi_j|^2 = 1$. Therefore $\bar{n}\Delta\omega/2\pi$ is the pump pulse train average power, and here $\bar{n}$ is the number of photons per pulse. Each pump spectral component is modulated by the refractive-index fluctuations, characterized by the phase-noise parameter $\rho(\delta)$, which is proportional to the ratio of phase noise to fiber nonlinearity, such that the phase fluctuation quadrature of a continuous wave beam would receive an excess noise power relative to the vacuum-noise level given by $\langle |X_\phi(\delta)|^2 \rangle = 2r\rho(\delta)$, where $X_\phi(\delta) = -i(a_+ - a_-^\dagger)$ is the usual quadrature amplitude for phase fluctuations of a cw beam at Fourier frequency δ.[3,19,20] Here a_+ and a_- are annihilation operators for modes at frequencies $\omega_0+\delta$ and $\omega_0-\delta$, respectively, and r is a parameter which characterizes the effective strength of nonlinear effects (i.e., squeezing: hence the term squeeze parameter). As defined and used in this paper, the quantity r is proportional to the *average* pump power, the fiber nonlinear susceptibility, and the propagation distance, and is defined by

$$r = (3\omega_0\chi^{(3)}/4nc)|E_p|^2 l \ , \tag{3.2}$$

where $\chi^{(3)}$ is the usual third-order nonlinear susceptibility. E_P is the pump field strength, and l is the fiber length.

For a train of pulses, refractive-index fluctuations produce phase-modulation sidebands on each spectral component, and, since the phase-noise bandwidth is likely to be large compared with the pulse repetition rate, these sidebands will overlap with many other spectral components of the pulse train to produce contributions to the low-frequency (compared to the pulse repetition rate) phase noise from high-frequency portions of the refractive-index fluctuation spectrum. In fact, refractive-index fluctuations at frequencies near every multiple of the pulse repetition rate, $\Delta\omega/2\pi$, will all contribute to observed phase noise near zero frequency. As the pulse is shortened by adding more spectral components thus increasing its bandwidth, the low-frequency phase noise will thus increase, assuming that the average power of the pulse train is held constant, until the bandwidth of the pulses becomes larger than the bandwidth of the refractive-index fluctuations. Beyond that point, the phase noise ceases to increase as the pulse is shortened and depends only on the total mean-square phase fluctuations imposed on the beam.

To be more quantitative, consider hyperbolic secant pulses with bandwidth σ_ω, i.e.,

$$\phi_j = (\pi\Delta\omega/4\sigma_\omega)^{1/2} \mathrm{sech}(j\pi\Delta\omega/2\sigma_\omega) \ , \tag{3.3}$$

corresponding to a pulse width $t_0 = \sigma_\omega^{-1}$. We describe the effect of the refractive-index fluctuations in terms of quadrature operators $X_A^j(\delta) = a_{+j} + a_{-j}^\dagger$ and $X_\phi^j(\delta) = -i(a_{+j} - a_{-j}^\dagger)$ corresponding to amplitude and phase modulation, respectively, of the jth spectral component of the pulse train. The annihilation operators $a_{\pm j}$ are defined for modes at frequencies $\omega_0 + j\Delta\omega \pm \delta$ in an interaction picture which tracks the phase of the jth pump component.[3,20] The overlapping phase-modulation sidebands result in the following expressions:

$$X_A^j(\delta) = \left[\frac{\bar{n}\Delta\omega}{2\pi} \right]^{1/2} \sum_{n=1}^{\infty} \{ [R(n\Delta\omega+\delta) + R(n\Delta\omega-\delta)](\phi_{j-n} - \phi_{j+n}) \} \ , \tag{3.4}$$

$$X_\phi^j(\delta)=-i\left[\frac{\bar{n}\Delta\omega}{2\pi}\right]^{1/2}\left[2\phi_j R(\delta)+\sum_{n=1}^{\infty}[R(n\Delta\omega+\delta)-R(n\Delta\omega-\delta)](\phi_{j-n}+\phi_{j+n})\right] . \tag{3.5}$$

Here $R(\delta)$ is a phase-modulation index operator for Fourier frequency δ.

It will be assumed that the noise is detected with a train of local oscillator pulses which are phase-shifted and attenuated replicas of the pump pulses, yielding photocurrent given by

$$I(\delta,\theta)=\left[\frac{n_{\mathrm{LO}}\Delta\omega}{2\pi}\right]^{1/2}\sum_{j=-\infty}^{\infty}\phi_j[X_A^j(\delta)\cos\theta+X_\phi^j(\delta)\sin\theta] , \tag{3.6}$$

where n_{LO} and θ are the photon number per pulse and phase shift of the local oscillator. Since $X_A \equiv\sum_j\phi_j X_A^j=0$, there is no net amplitude modulation of the pulse train. On the other hand, for $\theta=\pi/2$, the observed photocurrent fluctuations are proportional to $\langle|X_\phi|^2\rangle$, where $X_\phi\equiv\sum_j\phi_j X_\phi^j$:

$$\begin{aligned}\langle|I(\delta,\theta=\pi/2)|^2\rangle&=\left[\frac{n_{\mathrm{LO}}\Delta\omega}{2\pi}\right]\langle|X_\phi|^2\rangle\\&=r\left[\frac{n_{\mathrm{LO}}\Delta\omega}{2\pi}\right]\sum_{n=0}^{\infty}|f_n|^2[\rho(n\Delta\omega+\delta)\\&\quad+\rho(n\Delta\omega-\delta)] ,\end{aligned} \tag{3.7}$$

where

$$\begin{aligned}f_n&\equiv\sum_{j=-\infty}^{\infty}\phi_j(\phi_{j-n}+\phi_{j+n})\\&=2(n\pi\Delta\omega/2\sigma_\omega)\mathrm{csch}[n\pi\Delta\omega/2\sigma_\omega] .\end{aligned}$$

The phase-noise parameter ρ is defined by $\langle|R(\delta)|^2\rangle(\bar{n}\Delta\omega/2\pi)\equiv r\rho(\delta)$, where the squeeze parameter r is defined in Eq. (3.2). The quantity ρ is thus proportional to the ratio of the mean-square refractive-index fluctuation density at frequency δ to the nonlinear susceptibility.

To proceed further, it is useful to introduce a simple model for the spectrum of the phase-noise parameter δ. Since the fine structure of GAWBS will be washed out by the many overlapping spectral components produced by the multifrequency pump, it is sufficient to adopt a Lorentzian spectrum characterized by strength g and bandwidth γ:

$$\rho(\delta)=\frac{g}{1+\delta^2/\gamma^2} . \tag{3.8}$$

This Lorentzian spectrum is shown as the dashed curve in Fig. 1 for comparison with the typical fiber phase-noise spectrum. This model spectrum ignores the large phase-noise singularity near $\delta=0$ because of the $1/f$ contribution. This is not a serious omission, since we anticipate that the noise spectrum will be homodyne detected, by phase shifting the coherent field of the pulse relative to the stochastic field by reflecting the pulses from a phase-shifting interferometer[3] with free spectral range matched to the pulse-train repetition rate, and thus the $1/f$ part of the phase noise will be filtered out.[21] As discussed above, we expect the bandwidth in real frequency units to be on the order of tens of GHz, and should be approximately inversely proportional to the core diameter a. The strength g should characterize the average GAWBS spectral density near $\delta=0$, and this depends on the diameter of the fiber cladding, A, with $A\sim100$ μm. The spacing between GAWBS peaks scales as A^{-1}, while the scattering strength (area) of a given peak scales as A^{-2}.[7] Thus we expect $g\propto A^{-1}$, and the integrated area under the function $\rho(\delta)\propto(aA)^{-1}$. As $a, A\to\infty$, we approach the bulk case and forward Brillouin scattering vanishes, as expected.

Consider a measurement of noise at low frequencies (relative to the repetition rate, which for a typical mode-locked laser is of the order of 100 MHz). Since the GAWBS cutoff is of the order of tens of GHz, we have the relationship $\delta<\Delta\omega\ll\gamma,\sigma_\omega$. Two limits are obtained depending on the relative magnitudes of the GAWBS bandwidth and the pulse bandwidth. If $\gamma\ll\sigma_\omega$, then f_n is constant over the range that ρ is nonzero, and

$$\langle|I(\delta,\theta=\pi/2)|^2\rangle=\left[\frac{n_{\mathrm{LO}}\Delta\omega}{2\pi}\right](2\pi gr)(\gamma/\Delta\omega) . \tag{3.9}$$

In this case the noise is proportional to the area under $\rho(\delta)$, i.e., to the total mean-square phase fluctuations, and is independent of σ_ω and thus independent of the pulse width. It should also be noted that this result is proportional to the average power.

On the other hand, when $\gamma\gg\sigma_\omega$, $\rho(\delta)\simeq g$ over the entire pulse bandwidth, and

$$\begin{aligned}\langle|I(\delta,\theta=\pi/2)|^2\rangle&=\left[\frac{n_{\mathrm{LO}}\Delta\omega}{2\pi}\right]2gr\sum_{n=0}^{\infty}|f_n|^2\\&=\left[\frac{n_{\mathrm{LO}}\Delta\omega}{2\pi}\right]2gr\left[\frac{13.16\sigma_\omega}{\pi\Delta\omega}\right] .\end{aligned} \tag{3.10}$$

In this case the noise is proportional to the peak power and therefore increases as the pulse width is decreased, while maintaining constant average power.

In the case that $\gamma\ll\sigma_\omega$, the dependence of the excess thermal phase noise on the pulse-train average power and independence on the pulse width confirms the results of Sec. II B. By decreasing the pulse width, the effective nonlinearity increases as reflected in the quadratic decrease in z_0, while the average power and also the phase noise only scales linearly. To verify quantitatively the expected quantum-noise reduction, we now consider the propagation equation for the soliton field and the fluctuations, including the thermal phase noise.

IV. SOLITON PROPAGATION: THE STOCHASTIC NONLINEAR SCHRÖDINGER EQUATION

In general, the spectral and temporal structure of a coherent pulse propagating in an optical fiber will be modified by self-phase-modulation, which tends to generate new spectral components, and by the group-velocity dispersion of the fiber, which tends to broaden the pulse temporally. These processes can be accurately described by the nonlinear Schrödinger equation (NLSE), well known in the study of nonlinear pulse propagation in fibers.[17] For wavelengths in the anomalous dispersion region of a fiber, the fundamental soliton solution to the NLSE exists in the form of a hyperbolic secant pulse, which for classical coherent light propagates in the absence of loss without distortion.

The role of quantum noise in soliton propagation is an area of considerable recent theoretical activity.[12,22] Our quantum treatment of this problem[12] consists of writing the field in terms of the positive-P representation and deriving stochastic differential equations for the associated c-number field amplitudes, $\phi(\tau,\zeta)$, where τ and ζ are the local time and propagation distance, scaled in the customary way.[17] These stochastic differential equations contain noise sources which take proper account of the quantum and thermal noise and have a form similar to the NLSE:

$$\frac{\partial\phi}{\partial\zeta}=\left[\frac{i}{2}\left[\frac{\partial^2}{\partial\tau^2}-1\right]+i\phi^\dagger\phi+(i/\bar{n})^{1/2}\eta(\tau,\zeta)\right]\phi\ . \tag{4.1}$$

Here, $\bar{n}=|k''|/\chi t_0$ is the characteristic photon number per soliton, and $\bar{n}\langle\phi^\dagger\phi\rangle/t_0$ is the dimensionless photon flux in the fiber. The dimensionless variables, $\tau=t/t_0$ and $\zeta=z/z_0$, are defined in terms of a characteristic time t_0 and length $z_0=t_0^2/|k''|$ as defined earlier. The Kerr coefficient $\chi=n_2\hbar\omega_0^2/cA$, where n_2 is the intensity-dependent refractive index, and A is the effective cross-sectional area of the fiber mode. The noise source $\eta(\tau,\zeta)$ contains a δ-correlated quantum-noise term and an exponentially decaying thermal-noise term. Explicitly, this noise source is defined by the following moments:

$$\begin{aligned}\langle\eta(\tau_1,\zeta_1)\eta(\tau_2,\zeta_2)\rangle&=\langle\eta^\dagger(\tau_1,\zeta_2)\eta^\dagger(\tau_2,\zeta_2)\rangle^*\\&=\delta(\zeta_1-\zeta_2)\delta(\tau_1-\tau_2)+iG(\tau_1-\tau_2,\zeta_1-\zeta_2)\ ,\end{aligned} \tag{4.2}$$

$$\langle\eta(\tau_1,\zeta_1)\eta^\dagger(\tau_2,\zeta_2)\rangle=G(\tau_1-\tau_2,\zeta_1-\zeta_2)\ , \tag{4.3}$$

where $G(\delta\tau,\delta\zeta)$ is the real-valued scaled correlation function for the fluctuating refractive index at (τ,ζ) and $(\tau+\delta\tau,\zeta+\delta\zeta)$. In terms of the index fluctuations, $\delta n(\tau,\zeta)$, we have

$$\begin{aligned}&G(\tau_1-\tau_2,\zeta_1-\zeta_2)\\&\quad=\frac{1}{\chi}\left[\frac{\omega_0}{\bar{n}\omega'}\right]^2 z_0t_0\langle\delta n(\tau_1,\zeta_1)\delta n(\tau_2,\zeta_2)\rangle\ .\end{aligned} \tag{4.4}$$

Here $\omega'=\partial\omega/\partial k$ is the group velocity of the pulse.

We note the refractive-index fluctuations as being local but having exponentially decaying time correlations. Hence we take

$$\langle\delta n(\tau_1,\zeta_1)\delta n(\tau_2,\zeta_2)\rangle=\frac{\Gamma\gamma}{2z_0t_0}\delta(\zeta_1-\zeta_2)e^{-\gamma|\tau_1-\tau_2|}\ . \tag{4.5}$$

The physical decay rate is thus γ/t_0, which is fixed for a given fiber, and Γ characterizes the strength of the index fluctuations. Our dimensionless phase-fluctuation parameters are defined from here on by γ and

$$g\equiv\frac{\Gamma}{\chi}\left[\frac{\omega_0}{\bar{n}\omega'}\right]^2\ . \tag{4.6}$$

Thus phase noise due to GAWBS is modeled by a Lorentzian; i.e., $\rho(\delta)=(g\gamma^2)/(\delta^2+\gamma^2)$, where the parameter g corresponds to the phase-noise parameter used in the analysis of earlier cw fiber-squeezing experiments.[3] Based on our continuous-wave fiber-squeezing experiments and the scaling of GAWBS intensity with pump wavelength and fiber geometry,[7] we estimate $g\sim 5$ for a typical plastic-jacketed fiber at $\lambda=1.55$ μm and a temperature of 2 K. The value of the GAWBS bandwidth is unknown, but probably is near 20 GHz, yielding $\gamma<1$ for a soliton pulse width t_0 of about 10 psec or less.

The stochastic nonlinear Schrödinger equation can be linearized about the classical soliton solution, yielding Fourier domain equations for the propagation of the stochastic part of the field and its correlations.[12] Field correlations of the form

$$S_{ij}(\omega_1,\omega_2,\zeta)\equiv\langle\delta\phi_i(\omega_1,\zeta)\delta\phi_j(\omega_2,\zeta)\rangle\ ,$$

where $\delta\phi_1=\phi-\langle\phi\rangle$ and $\delta\phi_2=\phi^\dagger-\langle\phi^\dagger\rangle$, can thus be numerically propagated.

Homodyne detection of the noise spectrum would be accomplished by phase shifting the coherent field of the pulse relative to the stochastic fields, e.g., by reflection from a phase-shifting interferometer[3] matched to the pulse repetition rate. This technique also eliminates local oscillator phase jitter due to phase noise within the interferometer bandwidth, e.g., from microscopic pickup by the fiber or the low-frequency $1/f$ refractive-index fluctuations.

If $\phi_j^0\exp(i\theta)$ are the local oscillator spectral components, the detected photocurrent noise spectrum relative to the vacuum is given by

$$V(j\Delta\omega)=\Delta\omega\sum_{k,l}\phi^0_{j-l}\phi^0_{k-j}[S_{12}(l\Delta\omega,-k\Delta\omega)+S_{12}(-k\Delta\omega,l\Delta\omega)+e^{i2\theta}S_{11}(l\Delta\omega,-k\Delta\omega)+e^{-i2\theta}S_{22}(l\Delta\omega,-k\Delta\omega)]\ . \tag{4.7}$$

V. NUMERICAL RESULTS

The equations for the propagation of the correlations S_{ij} were numerically integrated on a computer for several values of g on the order of that estimated to be appropriate for a fiber designed for a soliton wavelength near 1.5 μm and cooled to 2 K. Simulations were run for bandwidth γ ranging from 0.1 in normalized frequency units to $\gamma=3$. To ensure convergence, the step size was shortened until no further improvement was noted over the range of propagation distances chosen, and the mesh size in the frequency dimension was similarly decreased to verify the accuracy of the results. Most of the runs covered propagation distances up to $\zeta=8$ in 200–500 steps, and a frequency range of $\delta=\pm 8$ with a mesh of 81 points. This was sufficient to ensure convergence in all cases.

The squeezing spectrum was calculated from Eq. (4.7), and the resulting squeezing spectrum for $g=0$ is shown in Fig. 2. The local oscillator spectrum ϕ_j^0 corresponds for this calculation to a hyperbolic secant pulse, with $\sigma_\omega=1$, i.e., a phase-shifted replica of the soliton. Such a local oscillator pulse would be readily available in a laboratory soliton-squeezing experiment, and our results show that it gives monotonically decreasing noise in the squeezed quadrature. The consequences of our using other pulse widths and Gaussian pulse shapes were also investigated, and will be discussed below. The local oscillator phase, $\theta_{\min}(\delta)$, required to give minimum noise, is dependent on the noise frequency δ. For the squeezing spectra displayed here it is assumed that at each value of δ the phase is adjusted to this optimum value, shown in Fig. 3. as a function of δ and propagation distance, ζ.

From Fig. 2 it is seen that at very small propagation distances the noise is squeezed over the entire soliton bandwidth. However, as the pulse continues down the fiber, the squeezing is fully developed only near zero frequency; while noise at frequencies near unity or greater in normalized units is amplified for all quadratures. In a Kerr medium, the amplitude noise is not modified by the nonlinearity. Rather the phase noise grows as a result of self-phase-modulation, and the squeezing arises as a result of the quantum correlation between this phase noise and the amplitude noise. At high frequencies, $\delta \geq 1$, and propagation distances $\zeta \geq 1$, dispersion plays a role, converting the phase noise into amplitude noise at a rate comparable or greater than the rate it is generated by self-phase-modulation. This feeds the noise back into the amplitude quadrature, resulting in amplification of the noise rather than squeezing. This phenomenon is demonstrated by Fig. 4, which shows the noise variance relative to the vacuum or shot-noise level for the pure amplitude-

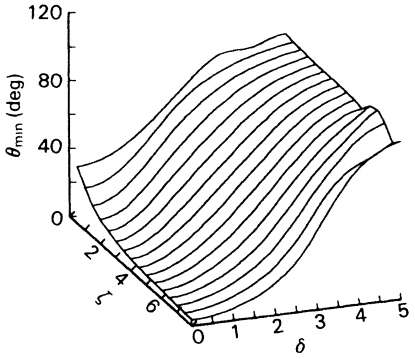

FIG. 3. The local oscillator phase necessary to obtain the minimum noise shown in Fig. 1 is plotted (in deg) as a function of scaled propagation distance and scaled frequency.

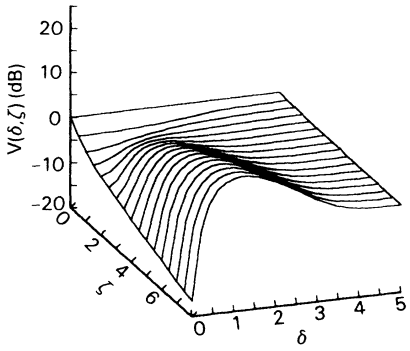

FIG. 2. Soliton-squeezing spectrum for optimum phase with $g=0$. The δ and ζ axes are in scaled soliton units, while the vertical axis is the noise variance in dB relative to the vacuum-noise level.

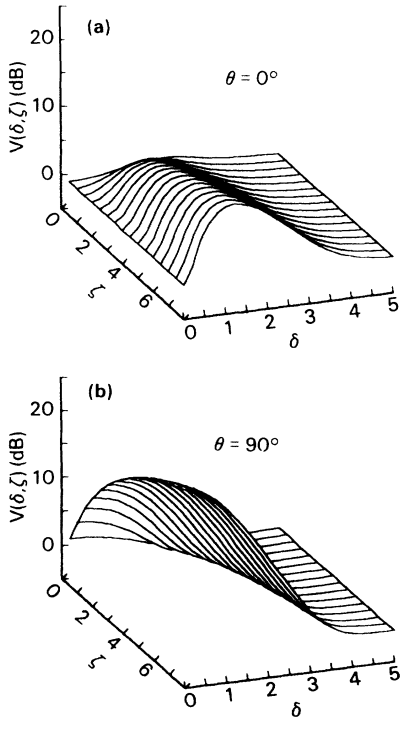

FIG. 4. The noise power for the (a) amplitude-noise quadrature, $\theta=0$, and for the (b) phase-noise quadrature, $\theta=\pi/2$, is plotted as a function of scaled propagation distance and scaled frequency, for $g=0$.

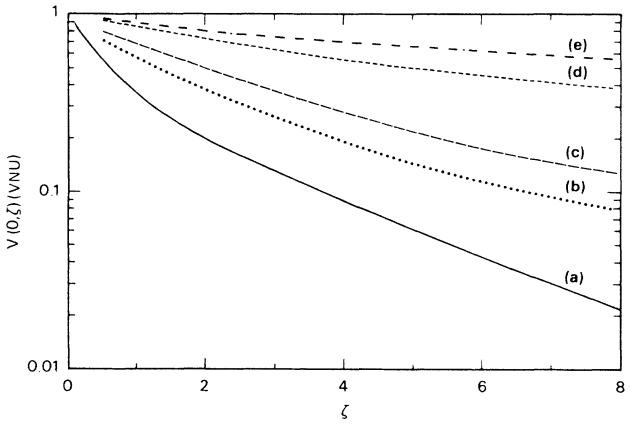

FIG. 5. Noise power relative to vacuum at $\delta=0$. Curve (a), $g=0$; curves (b), (d) and (e) $g=5$ and $\gamma=0.1$, 1, and 3, respectively. Curve (c) noise power at $\delta=0$ for both $g=10$, $\gamma=0.1$ and $g=5$, $\gamma=0.2$.

noise quadrature [$\theta=0$, Fig. 4(a)] and for the pure phase-noise quadrature [$\theta=\pi/2$, Fig. 4(b)]: The phase is seen to increase uniformly over the entire soliton spectrum, while the amplitude noise remains at the vacuum level at $\delta=0$, but grows at the higher frequencies because of dispersion.

The effect on the squeezing spectrum of introducing thermal phase noise is shown in Figs. 5–8. As described above and shown in Fig. 1, the phase noise is modeled as a Lorentzian spectrum, with $\rho(\delta)=g/(1+\delta^2/\gamma^2)$. In Fig. 5, we plot the noise variance relative to the vacuum-noise level at $\delta=0$, for $g=5$, or 10, and various values of the bandwidth γ. It can be seen that in the limit that $\gamma \ll 1$, the thermal phase noise has relatively little effect on the squeezing. We also note that the two sets of phase-noise parameters ($g=10$, $\gamma=0.1$, and $g=5$, $\gamma=0.2$) both yield curve (c) in Fig. 5 to within the accuracy of the plot, demonstrating that, in this limit, the

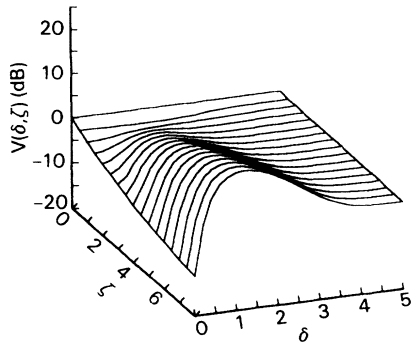

FIG. 6. Noise power relative to the vacuum level as a function of scaled distance and scaled frequency for thermal-noise parameters of $g=5.0$ and $\gamma=0.1$. As before, the noise power is plotted in dB for local oscillator phase chosen to minimize the noise at each frequency.

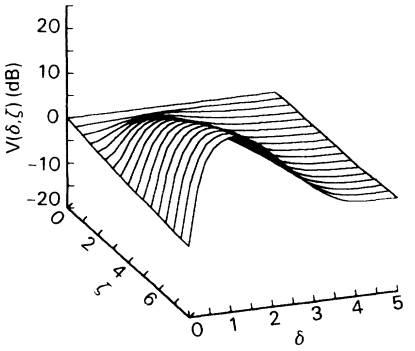

FIG. 7. Noise power relative to the vacuum level for thermal-noise parameters $g=0.5$ and $\gamma=1$.

noise reduction depends only on the total area under the thermal noise spectrum, i.e., on the total rms thermal phase variation.

In a real experiment, the magnitude of g is determined partly by the structure of the fiber, and it can be varied mainly by control of the temperature.[3,8,13] The bandwidth γ can be varied by varying the soliton bandwidth, i.e., the pulse width t_0. As the pulse width is varied, the characteristic length z_0 varies as t_0^{-2}. In view of the scaling properties of the squeezing and phase noise discussed above, it is instructive to replot curve (c) for $g=5$ and $\gamma=0.2$ and (d) for $g=5$ and $\gamma=1$, without rescaling the propagation distance axis. This is done in Fig. 9, where the horizontal axis corresponds to physical distance in meters, assuming that $\gamma=0.2$ corresponds to a pulse width of 1 psec and $z_0=25$ m, appropriate for typical group-velocity dispersion at 1.55 μm. The curve for $g=0$ is also replotted for the shorter pulses to demonstrate the much greater rate of squeezing for shorter soliton pulses. From this figure it is clear that the main advantage to be gained from reduction of the pulse width is an increase in the rate of squeezing rather than any decrease in the effect of the phase noise. This is emphasized by Fig. 10, in which we plot the phase noise ($\theta=\pi/2$) for $\gamma=0.2$ and 1, but for $g=200$, chosen so that the thermal phase noise, rather than the nonlinearly generated phase

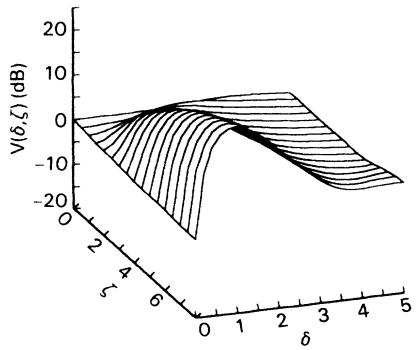

FIG. 8. Noise power relative to the vacuum level for thermal-noise parameters $g=5.0$ and $\gamma=3$.

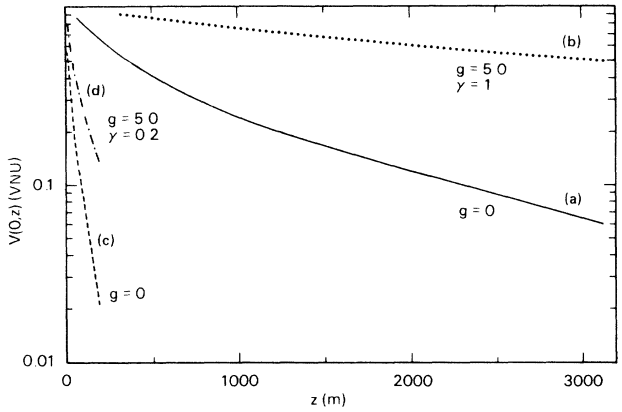

FIG. 9. Noise variance in VNU for $\delta=0$ as a function of propagation distance in meters. Curves (*a*) and (*b*), for $g=0$ and for $g=5$, $\gamma=1$, respectively, are plotted assuming a 5-psec pulse width and $z_0=625$ m, which corresponds to a dispersion parameter which is typical for $\lambda=1.55$ μm. Curves (*c*) and (*d*) correspond to $g=0$ and to $g=5$, $\gamma=0.2$, respectively, but with a soliton pulse width of 1 psec, a factor of five shorter. Thus $z_0=25$ m, and squeezing occurs over a much shorter propagation distance. All four curves correspond to a scaled propagation distance over the range from $\zeta=0$ to 8.

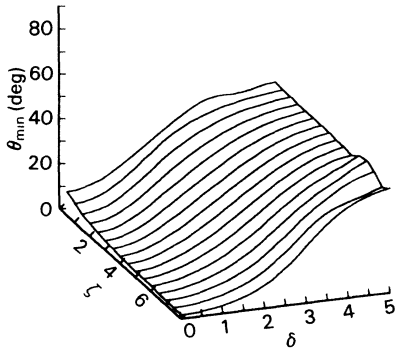

FIG. 11. Local oscillator phase necessary to obtain the minimum noise variance shown in Fig. 6, plotted as a function of scaled propagation distance and scaled frequency. Thermal-noise parameters are $g=5.0$ and $\gamma=0.1$.

noise, is completely dominant. It can be seen that the phase-noise variance grows faster for the shorter pulse because of the increased photon number required by the scaling of the fundamental soliton. [See Eqs. (2.11) and (3.9).]

We have also calculated the entire squeezing spectrum for a variety of values of g and γ. This is shown in Figs. 6–8, for $g=5$ and $\gamma=0.1$, 1, and 3, respectively. As the pulse propagates, dispersion converts the thermal phase noise into amplitude noise, and this enhances the noise amplification away from $\delta=0$. Since the thermal noise adds uncorrelated phase noise, the local oscillator phase shift $\theta(\delta)$ for best noise reduction is pushed in toward zero, as shown in Fig. 11.

Finally, we have investigated the use of both hyperbolic secant and Gaussian local oscillator pulses with various widths. The resulting noise reduction at $\delta=0$ is shown in Fig. 12 for several of these. LO pulses that are shorter than the soliton yield somewhat greater squeezing near zero frequency for short propagation distance, as might be expected from the argument that the greatest squeezing is near the peak of the pulse, where the instantaneous intensity is highest. However, for longer propagation distances, the noise continues to decrease monotonically only for the case of unity-width hyperbolic secant. For comparison, a cw beam with pump field

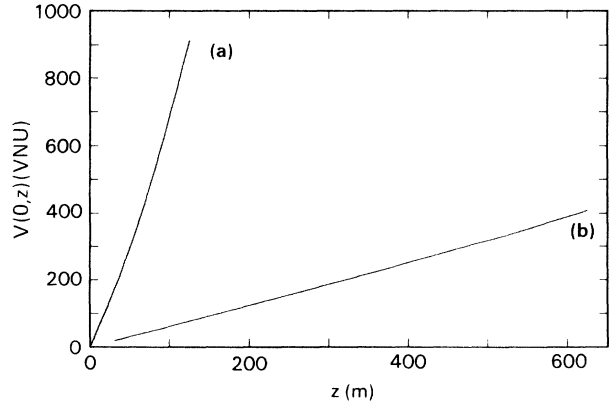

FIG. 10. Growth of the $\delta=0$ phase-noise quadrature ($\theta=\pi/2$) for $g=200$ and $\gamma=0.2$ [curve (*a*)] and 1 [curve (*b*)]. The propagation distance is plotted in meters for the same pulse widths and dispersion parameters as in Fig. 9, so that the two curves can be compared on the same physical distance scale. The thermal-noise magnitude is chosen large enough to dominate over phase noise due to self-phase-modulation in order to demonstrate the faster growth of thermal phase noise for shorter soliton pulses (which correspond to greater photon number).

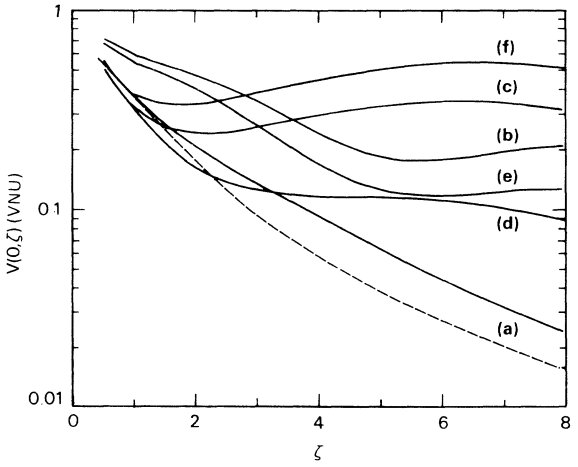

FIG. 12. Noise reduction in the squeezed quadrature at $\delta=0$ for a variety of local oscillator pulse widths and for both hyperbolic secant [curves (*a*)–(*c*)] and Gaussian [curves (*d*)–(*f*)] pulse shapes. The bandwidths of the local oscillator pulses are, in scaled soliton frequency units, (*a*) 1.0, (*b*) 0.5, (*c*) 2.0, (*d*) 1.0, (*e*) 0.5, and (*f*) 2.0. For these simple pulse shapes, the best choice is a hyperbolic secant of bandwidth 1.0. The dotted curve is the function $1+\zeta^2/2-\zeta(1+\zeta^2/4)^{1/2}$ (see text).

strength E_P gives, after propagation through a fiber of length l, a squeeze parameter r defined above in Eq. (3.2), corresponding in soliton units to a scaled propagation distance of $\zeta=2r$. The resulting noise power at $\delta=0$ relative to the vacuum is[23] $V_{cw}=1+2(\zeta/2)^2-2(\zeta/2)(1+(\zeta/2)^2)^{1/2}$, and this is plotted as the dotted curve in Fig. 12. Recent analytical results by Lai and Haus[22] indicate that the optimum local oscillator pulse shape is a more complicated function depending on propagation distance. With such a local oscillator, it may be possible to improve slightly upon the performance predicted for a simple hyperbolic secant local oscillator pulse.

VI. CONCLUSION

Probably the most important problem to be overcome to generate useful amounts of squeezing in an optical fiber is that of thermal fluctuations of the fiber refractive index and the resulting excess phase noise. These thermal fluctuations, originating in acoustic modes confined by the cylindrical fiber geometry, and in localized relaxation modes of groups of atoms (the so-called two-level modes), have limited all previous nonlinear quantum-optics experiments in optical fibers. To minimize the effect of this noise, we discuss the use of soliton pulses that are short compared with the inverse of the bandwidth of the phase noise, allowing significant squeezing to be obtained in fibers that are short compared with the propagation distance required for significant phase noise to accumulate.

In addition to the enhanced squeezing that is obtained as a result of the greater peak power of short pulses, the generation, propagation, and detection of squeezed pulses is of importance for sub-shot-noise time-resolved measurements, as well as in potential applications of nonclassical light to communications and optical computing.

We have given scaling arguments, verified by numerical solution of the stochastic nonlinear Schrödinger equation, to show that in the short-pulse limit substantial noise reduction below the vacuum level can be obtained with soliton pulses in a cryogenic optical fiber. The phase-noise bandwidth (and thus the necessary pulse width) is not known, although a reasonable estimate would put the bandwidth of the GAWBS spectrum at about 20 GHz, implying that pulses of the order of 1 psec are required.

It should be noted that, for pulses significantly narrower than 1 psec, Raman scattering from localized acoustic phonons may begin to add noise. The Raman-scattering cross section increases as frequency squared in the region from 1 to $\sim 100\ \mathrm{cm}^{-1}$, as shown by the dotted curve in Fig. 1. Also shown in Fig. 1 (the dot-dashed curve) is the spectrum of a soliton pulse, with width chosen to yield $\gamma=0.1$ with the GAWBS cutoff frequency chosen for this figure, i.e., 20 GHz. Although the hyperbolic secant falls off quite rapidly in the wings, a substantial fraction of the intensity could overlap the region where Raman scattering is becoming significant. The effect of Raman scattering on noise at the quantum level has not been considered in any detail, but it must be taken into account if extremely short pulses turn out to be necessary to circumvent the low-frequency thermal phase noise that is known from previous fiber-squeezing experiments.

ACKNOWLEDGMENTS

The work at IBM was supported in part by the Office of Naval Research. The authors are grateful to M. D. Levenson for many helpful discussions.

[1]See, for example, R. E. Slusher, B. Yurke, A. LaPorta, D. F. Walls, and M. D. Reid, J. Opt. Soc. Am. B **4**, 1453 (1987).

[2]L. A. Wu, M. Xiao, and H. J. Kimble, J. Opt. Soc. Am. B **4**, 1465 (1987).

[3]G. J. Milburn, M.D. Levenson, R. M. Shelby, S. H. Perlmutter, R. G. DeVoe, and D. F. Walls, J. Opt. Soc. Am. B **4**, 1476 (1987).

[4]M. W. Maeda, P. Kumar, and J. H. Shapiro, J. Opt. Soc. Am. B **4**, 1501 (1987).

[5]W. J. Kozlovsky, C. D. Nabors, R. C. Eckardt, and R. L. Byer, Opt. Lett. **14**, 66 (1989); C. D. Nabors, R. C. Eckardt, W. J. Kozlovsky, and R. L. Byer, *ibid.* **14**, 1134 (1989).

[6]S. Machida, Y. Yamamoto, and Y. Itaya, Phys. Rev. Lett. **58**, 1000 (1987); S. Machida and Y. Yamamoto, *ibid.* **60**, 792 (1988); W. H. Richardson and R. M. Shelby, *ibid.* **64**, 400 (1990).

[7]R. M. Shelby, M. D. Levenson, and P. W. Bayer, Phys. Rev. B **31**, 5244 (1985).

[8]S. H. Perlmutter, M. D. Levenson, R. M. Shelby, and M. B. Weissman, Phys. Rev. Lett. **61**, 1388 (1988).

[9]B. Yurke, P. Grangier, R. E. Slusher, and M. J. Potasek, Phys. Rev. A **35**, 3586 (1987).

[10]R. E. Slusher, P. Grangier A. LaPorta, B. Yurke, and M. J. Potasek, Phys. Rev. Lett. **59**, 2566 (1987).

[11]B. L. Schumaker, J. Opt. Soc. Am. A **3**, P38 (1986).

[12]S. J. Carter, P. D. Drummond, M. D. Reid, and R. M. Shelby, Phys. Rev. Lett. **58**, 1841 (1987); P. D. Drummond and S. J. Carter, J. Opt. Soc. Am. B **4**, 1565 (1987); P. D. Drummond, S. J. Carter, and R. M. Shelby, Opt. Lett. **14**, 373 (1989).

[13]S. H. Perlmutter, M. D. Levenson, R. M. Shelby, and M. B. Weissman, Phys. Rev. B (to be published).

[14]This normalization is discussed in more detail in the Appendix of Ref. 13. It provides a very useful measure of photocurrent noise power, particularly where excess noise sources such as light scattering are concerned. When expressed in VNU, the noise power is *independent* of detection parameters, such as bandwidth, amplifier gain, and local oscillator power, is an absolute measure since it is expressed in terms of a fundamental quantity, and is operationally convenient for laboratory measurements.

[15]See S. Hunklinger and M. v. Schiekfus, in *Amorphous Solids—Low-Temperature Properties,* Vol. 24 of *Topics in Current Physics,* edited by W. A. Philips (Springer-Verlag, Berlin, 1981).

[16]P. Dutta and P. M. Horn, Rev. Mod. Phys. **53**, 497 (1981); M. B. Weissman, *ibid.* **60**, 537 (1988).
[17]L. F. Mollenauer, Philos. Trans. R. Soc. London, Ser. A **315**, 435 (1985).
[18]R. M. Shelby (unpublished).
[19]C. M. Caves and B. L. Schumaker, Phys. Rev. A **31**, 3068 (1985).
[20]M. D. Levenson and R. M. Shelby, J. Mod. Opt. **34**, 775 (1987).
[21]T. A. B. Kennedy (private communication); S. J. Carter and P. D. Drummond (unpublished).
[22]Y. Lai and H. A. Haus, Phys. Rev. A **40**, 844, 854 (1989); H. A. Haus and Y. Lai, J. Opt. Soc. Am. B **7**, 386 (1990).
[23]M. D. Levenson, R. M. Shelby, and S. H. Perlmutter, Opt. Lett. **10**, 514 (1985).